

COMMISSIONS 27 AND 42 OF THE IAU  
INFORMATION BULLETIN ON VARIABLE STARS

Number 6xxx

Konkoly Observatory  
Budapest  
01 February 2013  
*HU ISSN 0374 – 0676*

**RR LYRAE STARS IN THE GCVS OBSERVED BY THE  
QATAR EXOPLANET SURVEY**

BRAMICH, D.M.<sup>1</sup>; ALSUBAI, K.A.<sup>1</sup>; ARELLANO FERRO, A.<sup>2</sup>; PARLEY, N.R.<sup>1,3</sup>; COLLIER  
CAMERON, A.<sup>3</sup>; HORNE, K.<sup>3</sup>; POLLACCO, D.<sup>4</sup>; WEST, R.G.<sup>4</sup>

<sup>1</sup> Qatar Environment and Energy Research Institute, Qatar Foundation, Tornado Tower, Floor 19, P.O. Box 5825, Doha, Qatar

<sup>2</sup> Instituto de Astronomía, Universidad Nacional Autónoma de México, Ciudad Universitaria CP 04510, México

<sup>3</sup> SUPA, School of Physics and Astronomy, University of St Andrews, North Haugh, St Andrews, Fife, KY16 9SS, UK

<sup>4</sup> Department of Physics, University of Warwick, Coventry, CV4 7AL, UK

## 1 Abstract

We used the light curve archive of the Qatar Exoplanet Survey (QES) to investigate the RR Lyrae variable stars listed in the General Catalogue of Variable Stars (GCVS). Of 588 variables studied, we reclassify 14 as eclipsing binaries, one as an RS Canum Venaticorum-type variable, one as an irregular variable, four as classical Cepheids, and one as a type II Cepheid, while also improving their periods. We also report new RR Lyrae sub-type classifications for 65 variables and improve on the GCVS period estimates for 135 RR Lyrae variables. There are seven double-mode RR Lyrae stars in the sample for which we measured their fundamental and first overtone periods. Finally, we detect the Blazhko effect in 38 of the RR Lyrae stars for the first time and we successfully measured the Blazhko period for 26 of them.

## 2 Introduction

The Qatar Exoplanet Survey (QES; Alsubai et al. 2013) is discovering hot Jupiters (Qatar-1b, Alsubai et al. 2011; Qatar-2b, Bryan et al. 2012) and aims to discover hot Saturns and Neptunes that transit in front of relatively bright host stars (8-15 mag). The survey operates a robotic wide-angle multiple-camera system installed at the “New Mexico Skies” observing station in southern New Mexico, USA, and it has been in operation since mid-November 2009. The cameras, which operate without filters for maximum signal-to-noise (S/N), photometrically survey a target field of  $\sim 400$  square degrees repeatedly with a cadence of  $\sim 10$  minutes. Each target field is followed for  $\sim 3-4$  months continuously while it is visible at greater than  $30^\circ$  above the horizon. Each year a new set of target fields are designated.

The time-series images of each field are processed by a customised data pipeline (Sec. 4 of Alsubai et al. 2013) to calibrate the images, detect objects, perform astrometry, and extract photometry. Only objects successfully matched with stars in the US Naval Observatory CCD Astrograph Catalog (UCAC3; Zacharias et al. 2010) are considered further in order to avoid faint stars with very low S/N. A reference image, chosen as a best-seeing high-S/N image from the time series, is subtracted from each image in the time series using the image subtraction technique to create difference images (Alard & Lupton 1998; Bramich 2008; Bramich et al. 2013). Photometry is performed on the difference images using point spread function (PSF) fitting at the object positions with a spatially-variable PSF model. The output of this difference image analysis (DIA) is a set of object light curves in differential flux units (ADU/s). These light curves are converted to instrumental magnitudes using reference fluxes for each object as measured on the reference image. The photometric zero point for the reference image is determined using the UCAC3 magnitudes and this is used to calibrate the light curve magnitudes on an absolute scale with a scatter of  $\sim 0.1$  mag. The QES light curves are then stored in a data archive system and trend filtering algorithms are applied to them. However, since the application of trend filtering algorithms to variable star light curves risks distorting their shape, we opted to use the raw QES light curves from the archive (i.e. before detrending is applied) for the study of the variable stars in this paper.

With a typical photometric precision of  $\sim 1\text{-}2\%$  over the magnitude range 8-14, a high temporal cadence ( $\sim 10$  min) sustained over  $\sim 2\text{-}7$  hours in each 24-hour period, and a time baseline of  $\sim 3\text{-}4$  months, the QES light-curve archive is a potential gold mine for variability studies. As part of realising the full scientific potential of QES, we have started to investigate the variable star content of the archive. This short paper is the first in a series reporting our results. Here we investigate known RR Lyrae variables.

### 3 Sample Selection

We cross-matched UCAC3 with the 47969 variable stars in the General Catalogue of Variable Stars (GCVS4 - version 30/04/2013; Samus et al. 2009) using the CDS X-Match service<sup>1</sup>. The cross-match algorithm simply selects any GCVS star entries within a  $5''$  radius of any UCAC3 star. This resulted in 43009 matched entries, of which 42973 are unique. Retaining only the unique matches and filtering for variable star type, we obtained 6921 UCAC3 stars classified as RR Lyrae variables.

We then searched in the QES light-curve archive for these UCAC3 RR Lyrae stars and found that we had observed 752 objects in this list. We note that any object observed across multiple target fields and/or cameras will have multiple light curves in the QES archive. Since our analysis requires a reasonable number of data points in each light curve, we rejected light curves with fewer than 100 data points. Furthermore, due to the faint limit of the QES lying at  $\sim 17$  mag, we rejected any objects with UCAC3 aperture magnitudes fainter than 16.5. We were left with 724 objects with 2220 light curves.

We inspected plots of the phased (using the GCVS periods where available) and unphased light curves of our object sample. Since RR Lyrae variations have typical amplitudes of 0.1-1.3 mag, we could immediately identify 65 objects with multiple light curves where a subset of the light curves were not showing any variability. This occurs when the QES pipeline misidentifies an object and measures the wrong star, which tends to happen for relatively crowded objects towards the edge of a detector where camera dis-

<sup>1</sup><http://cdsxmatch.u-strasbg.fr/xmatch#tab=xmatch&>

tortions are not sufficiently well-modelled in the astrometric solution. For these cases we simply rejected the 143 light curves that failed to show the variations clearly visible in the remaining light curves for the same object. We also identified 136 objects for which none of their light curves showed variations above the noise level. We found that this was due either to the objects being very faint and therefore exhibiting a large scatter in their light curves, or to the object misidentification problem mentioned already. We rejected these objects from our sample, which left us with 588 photometrically variable objects with 1783 light curves.

## 4 Analysis And Results

Some variables in our data sample do not have GCVS period estimates and/or their GCVS classification as RR Lyrae variables is uncertain or does not distinguish between fundamental mode and first overtone pulsators. Hence our first step was to estimate the variable star periods using our light curve data. We applied the string-length method (Burke, Rolland & Boy 1970; Dworetzky 1983) to each of the 1783 light curves in our sample to search for periods in the range 0.1-500 d. For variables with multiple light curves, we adopted the period derived from the light curve with the best combination of the longest time span, the smallest noise, and the most data points (all light curve plots in this paper display this “best” light curve for clarity). We then phase-folded the light curves with our derived periods, and we checked the RR Lyrae classification of our variables.

Apart from being able to improve the GCVS periods and classifications for a large number of variable stars, we also found that some variables in our data sample are not RR Lyrae stars. Consequently we have reclassified these stars using the GCVS classification system described in Samus et al. (2009)<sup>2</sup>. To aid in our reclassification efforts, we searched the literature for previous studies of some of these variables. However, a full literature search for all of the variables in our data sample is outside of the scope of this paper, the purpose of which is to provide a set of concrete updates to the latest version of the GCVS. Therefore we cannot claim that all of our results are guaranteed to be new although we are sure that the majority of the information presented in this paper has not previously been reported in the literature.

Before reporting our results, we mention that due to the coarse pixel scale of the QES camera system (9.26 and 4.64 arcsec/pixel for the 200 and 400 mm lenses, respectively), a relatively high proportion of the variable stars in our sample are likely to be blended with another star. Hence the reference flux for such blended variables as measured on the reference image is systematically over-estimated which leads to artificially small amplitudes of variation in the corresponding light curves. Therefore, the amplitudes of our variable star light curves may be systematically too small in a number of cases when compared to light curves derived from higher resolution imaging data.

### 4.1 Stars that are not RR Lyrae variables

In Table 1, we report the reclassification of 21 variable stars. Our period estimates improve on the GCVS periods in all cases. We reclassify 14 of these variables as eclipsing binaries, where 13 of these are of the W Ursae Majoris-type. We plot the phased light curves of the eclipsing binaries in Figure 1 using the best light curve for each variable. Four eclipsing binaries (3UC191-025421, 3UC192-006598, 3UC247-041882 and 3UC308-105518) clearly

<sup>2</sup>See also <http://www.sai.msu.su/gcvs/gcvs/iii/vartype.txt>

show the O’Connell effect in our data, which is characterised by two maxima of different brightnesses (O’Connell 1951).

We find that the variable star 3UC205-101683, which is listed in the GCVS as an RR Lyrae star of unknown sub-type, is a known double-lined spectroscopic binary (Mathieu et al. 2003) showing X-ray emission (Belloni, Verbunt & Mathieu 1998) and classed as an RS Canum Venaticorum-type variable (van den Berg et al. 2002). We have updated the record for this star in Table 1, quoting the period derived from our best light curve spanning  $\sim 154$  days, which is more precise than the photometric periods quoted in the literature. The phased light curve for this star is shown in Figure 2. We note that the slight variations in the light curve shape and amplitude reported by van den Berg et al. (2002) are also detected in our light curve.

The variable star 3UC171-023140 is a Herbig Ae/Be star of spectral type B9e (Vieira et al. 2003) that exhibits irregular light variations (see Figure 3; Bernhard 2010). We were unable to find periodicity in our light curves for this object. Hence we reclassify this star as an irregular variable of early spectral type in Table 1.

We found that four of the variable stars in our sample are most likely classical Cepheids as opposed to RR Lyrae stars. Our new classifications for two of these stars (3UC208-318430 and 3UC225-131002) are based only on the period and the shape of the phased light curve (see Figure 4), which does not definitively distinguish them from other variable types in their period range. Hence our classifications for these two stars are tentative and marked with a colon “:” in Table 1. The variable star 3UC237-053427 was originally classified as a classical Cepheid by Schmidt & Gross (1990) and we confirm that it is most likely pulsating in the first overtone mode as indicated by its smaller pulsation amplitude and relatively symmetric phased light curve. The variable star 3UC268-064903 has also already been classified as a classical Cepheid by Wils, Lloyd & Bernhard (2006).

We also noticed that the variable star 3UC237-121450 has an unusually long period for an RR Lyrae. A literature search revealed that Wallerstein, Kovtyukh & Andrievsky (2009) found this star to be carbon-rich and of relatively high metallicity. These facts lead Andrievsky et al. (2010) to suggest that 3UC237-121450 is more likely to be a short-period type II Cepheid (or BL Her type variable). We adopt this tentative classification for this star in Table 1 and display the phased light curve in Figure 5.

## 4.2 RR Lyrae stars with new sub-type classifications

In Table 2, we report the new sub-type classifications for 61 RR Lyrae stars which have an unspecified or erroneous RR Lyrae sub-type classification in the GCVS. We list our period estimates in the table whenever they improve on the GCVS periods (52 cases). The new sub-type classifications are based on having considered the variable star periods and the phased light curve shapes and amplitudes. We note that some of the GCVS periods fail to properly phase our light curves, which may indicate period changes in these cases (e.g. 3UC167-134566). We clearly detect the Blazhko effect (amplitude and/or phase modulations; Blazhko 1907) in five of these RR Lyrae variables and this is the first detection of the effect in four of them (see the catalogue of known Galactic field Blazhko RR Lyrae stars in Skarka 2013). For 3UC191-097728, 3UC202-143008 and 3UC227-103944, we measure Blazhko periods of  $36.2 \pm 0.2$ ,  $40.0 \pm 0.6$  and  $65.6 \pm 1.2$  d, respectively, using the power

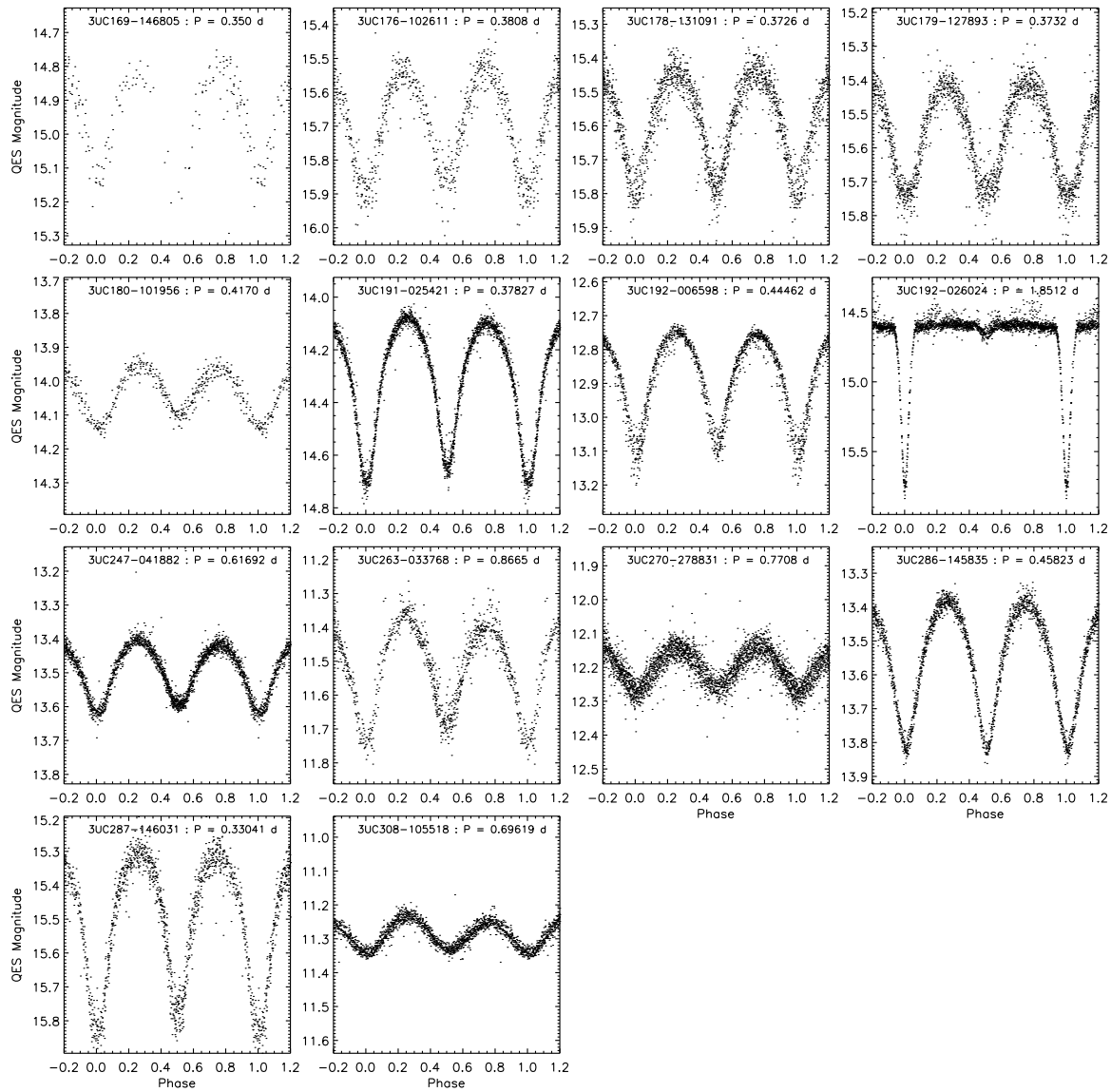


**Figure 1.** Phased light curves of the variable stars reclassified as eclipsing binaries. The magnitude range in each plot is 0.7 mag except for the stars 3UC191-025421 and 3UC192-026024 which have plots with magnitude ranges of 0.9 and 1.8 mag respectively.

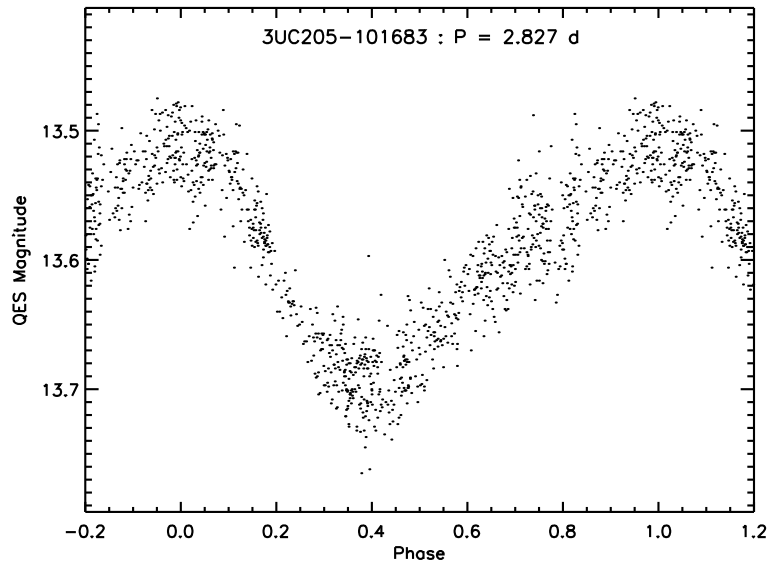


**Figure 2.** Phased light curve of the variable star 3UC205-101683 reclassified as a RS Canum Venaticorum-type variable.

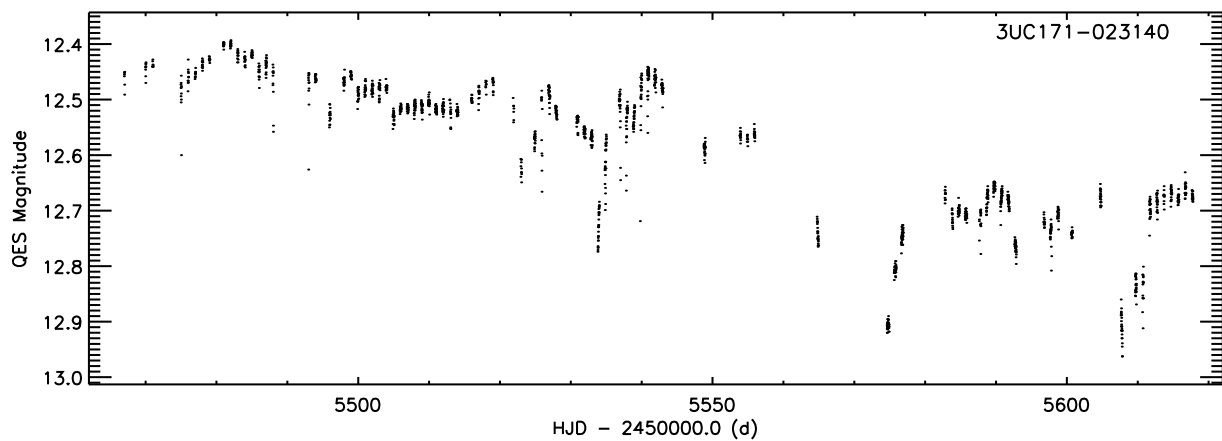


**Figure 3.** Light curve of the variable star 3UC171-023140 reclassified as an irregular variable of early spectral type.

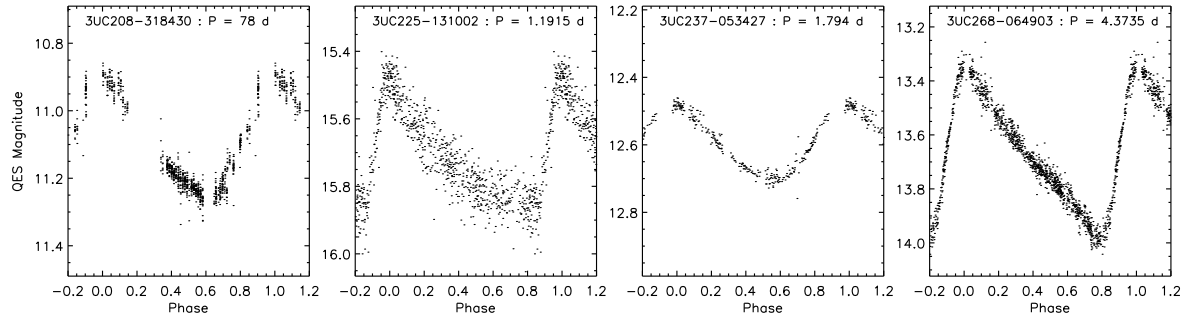


**Figure 4.** Phased light curves of the variable stars reclassified as classical Cepheids (or type I Cepheids). The magnitude range in each plot is 0.8 mag except for the star 3UC268-064903 which has a plot with a magnitude range of 1.0 mag.

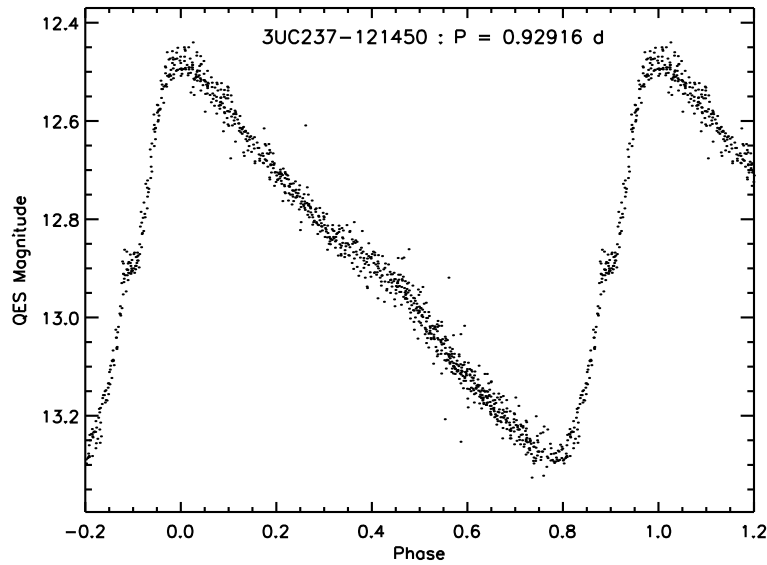


**Figure 5.** Phased light curve of the variable star 3UC237-121450 reclassified as a type II Cepheid.

**Table 1.** Variable stars reclassified as eclipsing binaries, RS Canum Venaticorum-type variables (or RS CVn), irregular variables of early spectral type, classical Cepheids (or type I Cepheids), and type II Cepheids. All of our period estimates improve on the GCVS periods and they are precise to the last decimal place quoted.

UCAC3 ID	GCVS ID	RA		Dec.		Variable Type		UCAC3		Period (d)	
		(J2000.0)	(J2000.0)	(J2000.0)	(J2000.0)	GCVS	This Work	Aperture Mag	GCVS	This Work	
169-146805	V1018 Oph	16 17 59.22	-05 56 55.3	RRC:	EW	15.244	0.3696396	0.350			
171-023140	UY Ori	05 32 00.31	-04 55 53.9	RR:	IA	12.456	-	-			
176-102611	V0482 Hya	08 27 38.98	-02 00 34.3	RRC:	EW	15.591	0.190393	0.3808			
178-131091	V0593 Vir	14 44 30.11	-01 28 26.2	RRC:	EW	15.473	0.228947	0.3726			
179-127893	V0533 Vir	14 12 38.56	-00 53 50.7	RRC:	EW	15.484	0.229537	0.3732			
180-101956	V0491 Hya	08 39 55.42	-00 03 50.4	RRC:	EW	14.055	0.263482	0.4170			
191-025421	V0651 Ori	05 32 46.49	+05 24 57.8	RR:	EW <sup>a</sup>	14.335	-	0.37827			
192-006598	HM Cet	02 07 31.42	+05 41 05.7	RRC	EW <sup>a</sup>	13.017	0.22232	0.44462			
192-026024	V1015 Ori	05 28 54.22	+05 39 27.7	RR:	EA	14.627	-	1.8512			
205-101683	AG Cnc	08 51 25.30	+12 02 56.5	RR:	RS <sup>b</sup>	13.684	0.313335	2.827 <sup>c</sup>			
208-318430	HU Peg	23 59 22.17	+13 47 11.5	RR	DCEP:	11.107	-	78 <sup>d</sup>			
225-131002	V0368 Her	17 10 31.13	+22 23 08.8	RRAB	DCEP:	15.627	0.543689	1.1915			
237-053427	CN Tau	05 58 09.42	+28 02 33.5	RRAB	DCEPS <sup>e</sup>	12.645	0.642062	1.794			
237-121450	UY CrB	16 06 21.77	+28 07 03.8	RR:	CWB: <sup>f</sup>	13.190	-	0.92916			
247-041882	DN Aur	05 07 59.86	+33 23 50.7	RRC	EW <sup>a</sup>	13.535	0.30846	0.61692			
263-033768	KN Per	03 22 35.64	+41 19 55.2	RRC	EW	11.615	0.433224	0.8665			
268-064903	V0421 Per	04 45 34.83	+43 34 22.2	RR	DCEP <sup>g</sup>	13.643	-	4.3735			
270-278831	V0660 And	23 27 52.08	+44 54 14.9	RRC	EW	12.147	0.38542	0.7708			
286-145835	V0997 Cyg	19 48 05.07	+52 51 16.3	RRC	EW	13.358	0.22892	0.45823			
287-146031	V1017 Cyg	19 56 15.81	+53 19 12.0	RR	EW	15.197	0.96	0.33041			
308-105518	V0414 Dra	18 53 30.15	+63 55 03.6	RRC:	EW <sup>a</sup>	11.306	0.348087	0.69619			

<sup>a</sup>Clear detection of the O’Connell effect (i.e. unequal brightness of the two maxima).

<sup>b</sup>Classification taken from van den Berg et al. (2002).

<sup>c</sup>Orbital period is 2.823094 d (Mathieu et al. 2003).

<sup>d</sup>This star has a single light curve in our data that spans  $\sim 195$  days (or  $\sim 2.5$  cycles).

<sup>e</sup>Originally classified as a classical Cepheid by Schmidt & Gross (1990).

<sup>f</sup>Classification taken from Andrievsky et al. (2010).

<sup>g</sup>Also classified as a classical Cepheid by Wils, Lloyd & Bernhard (2006).

spectrum analysis described in Section 4.5. For 3UC175-133697 we place a lower limit of 80 d on the Blazhko period. Finally we note that the light curve for 3UC236-044458 has a strange shape for an RR Lyrae star, although its period and amplitude are consistent with that of an RRC variable. The phase-folded light curves of all 61 variables are displayed in Figure 6.

### 4.3 Double-mode RR Lyrae stars

Seven of the variable stars in our sample are double-mode RR Lyrae stars pulsating simultaneously in the fundamental and first overtone modes. The GCVS classification for these stars is wrong in four cases. We checked the literature and all of these stars are known double-mode RR Lyrae stars. We used the program `period04` (Lenz & Breger 2005) to perform a frequency analysis on the best light curve for each star. Our results are reported in Table 3 where we list the correct classification for each star alongside the fundamental and first overtone periods that we measured. For all stars the period ratios between the two modes fall inside the expected range of 0.742-0.748 for this type of variable star (Cox, Hodson & Clancy 1983; Moskalik 2014). The corresponding light curves phased using the first overtone period are plotted in Figure 7.

### 4.4 RR Lyrae stars with improved periods

For the remaining 499 variables in our sample, the RR Lyrae classifications in the GCVS are correct. However, we have been able to improve on the GCVS period estimates for 83 variables. These stars along with their improved periods are listed in Table 4. Again, period changes in some of these variables may explain the differences between the GCVS



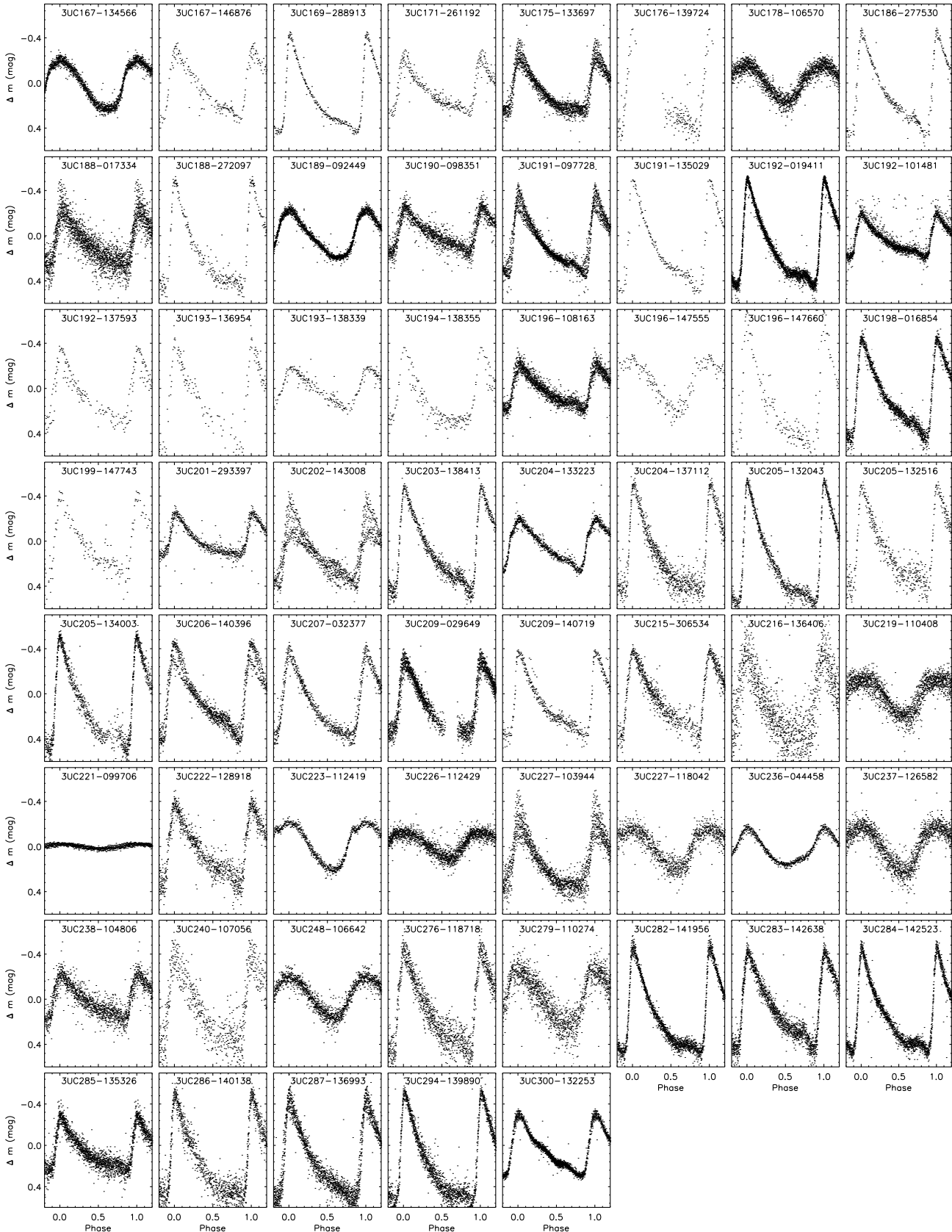


**Figure 6.** Phased light curves of the RR Lyrae stars with new sub-type classifications. The light curve magnitudes are plotted relative to the mean magnitudes and the same magnitude range of 1.3 mag is used in each plot. See Table 2 for the star brightnesses.

**Table 2.** RR Lyrae stars with new sub-type classifications. Where listed, our period estimates improve on the GCVS periods and they are precise to the last decimal place quoted.

UCAC3 ID	GCVS ID	RA		Dec.		Variable Type		UCAC3 Aperture Mag	Period (d)	
		(J2000.0)	(J2000.0)	(J2000.0)	(J2000.0)	GCVS	This Work		GCVS	This Work
167-134566	KW Lib	14 47 51.53	-06 34 45.9	RRAB	RRC	14.146	0.3143	0.31269		
167-146876	V0713 Oph	16 30 10.73	-06 48 02.1	RR	RRAB	14.384	-	0.6858		
169-288913	CH Aql	20 33 42.18	-05 38 49.3	RR	RRAB	13.894	0.38918702	-		
171-261192	V0909 Aql	20 21 59.39	-04 41 48.7	RR:	RRAB	14.758	0.5756	0.5766		
175-133697	FV Lib	14 48 50.96	-02 33 46.4	RR:	RRAB <sup>a,b</sup>	15.028	-	0.5404		
176-139724	CI Ser	16 13 41.43	-02 20 23.0	RR	RRAB	15.009	0.5383	0.5385		
178-106570	V0494 Hya	08 43 42.26	-01 20 17.0	RRC:	RRC	15.722	0.429765	-		
186-277530	EL Del	20 55 23.08	+02 57 35.3	RR	RRAB	14.285	0.595432	-		
188-017334	FV Ori	04 50 43.55	+03 47 35.1	RR	RRAB	16.486	0.55218	-		
188-272097	V0911 Aql	20 23 47.28	+03 36 49.2	RR	RRAB	15.897	-	0.46156		
189-092449	V0516 Hya	09 11 37.56	+04 02 30.4	RRAB:	RRC	13.150	0.346612	0.34666		
190-098351	UV Hya	09 38 15.28	+04 45 36.5	RR:	RRAB	14.153	-	0.7072		
191-097728	CY Hya	09 10 20.88	+05 20 51.1	RR	RRAB <sup>a,b</sup>	14.615	0.57693446	-		
191-135029	V1429 Oph	17 07 15.15	+05 15 08.2	RR	RRAB	14.187	-	0.3651		
192-019411	GO Ori	04 56 31.49	+05 35 33.7	RR	RRAB	15.092	-	0.53496		
192-101481	IU Hya	09 06 17.78	+05 45 45.3	RR:	RRAB	15.022	-	0.58033		
192-137593	V1053 Oph	16 54 46.95	+05 42 16.5	RR:	RRAB	14.921	4.03	0.578		
193-136954	V1056 Oph	16 59 23.92	+06 20 15.5	RR:	RRAB	16.249	-	0.593		
193-138339	V2598 Oph	17 05 43.58	+06 25 41.5	RRC	RRAB	14.428	0.38749054	0.634		
194-138355	V2620 Oph	16 51 05.97	+06 57 47.9	RRAB:	RRAB	15.329	0.456	-		
196-108163	BF Cnc	08 42 12.75	+07 48 38.0	RR	RRAB	15.928	-	0.58706		
196-147555	V1600 Oph	17 11 41.45	+07 32 11.1	RR	RRC	15.308	-	0.3080		
196-147660	V1060 Oph	17 12 16.20	+07 41 25.4	RR:	RRAB	15.475	-	0.4404		
198-016854	CK Tau	04 36 44.96	+08 54 24.4	RR	RRAB	14.808	-	0.6009		
199-147743	V0612 Her	16 45 06.95	+09 02 33.6	RR	RRAB	15.233	-	0.5807		
201-293397	KL Del	20 38 55.50	+10 29 03.2	RR:	RRAB	14.821	-	0.44110		
202-143008	V1061 Oph	17 14 29.98	+10 43 07.5	RR	RRAB <sup>a,b</sup>	14.966	-	0.58940		
203-138413	V1057 Oph	17 01 06.77	+11 03 17.6	RR	RRAB	15.398	-	0.61805		
204-133223	V0605 Her	16 40 41.80	+11 51 58.1	RR	RRAB	13.699	-	0.61129		
204-137112	V1322 Oph	17 03 43.25	+11 51 55.5	RR	RRAB	16.071	-	0.46955		
205-132043	V0546 Her	16 41 22.37	+12 25 10.8	RR	RRAB	14.706	-	0.467245		
205-132516	V0549 Her	16 44 03.55	+12 11 37.9	RR	RRAB	16.112	-	0.58518		
205-134003	V1122 Oph	16 53 44.99	+12 24 46.6	RR:	RRAB	16.128	-	0.50378		
206-140396	V0461 Her	17 10 49.32	+12 52 50.9	RR	RRAB <sup>a,b</sup>	13.264	0.51301	-		
207-032377	EX Tau	05 44 19.60	+13 27 54.3	RR	RRAB	15.159	-	0.5556		
209-029649	V0743 Ori	05 34 58.37	+14 25 26.9	RR	RRAB	15.722	-	0.5001		
209-140719	V0552 Her	17 30 11.83	+14 22 34.5	RR	RRAB	13.339	-	0.37846		
215-306534	HT Del	20 54 39.59	+17 12 02.2	RR	RRAB	16.117	0.362494	0.5699		
216-136406	BH Her	17 12 45.04	+17 42 31.0	RR:	RRAB	15.793	-	0.54514		
219-110408	MU Boo	14 48 14.73	+19 20 19.1	RRC:	RRC	14.205	0.320375	-		
221-099706	GN Cnc	09 16 04.44	+20 04 23.4	RR:	RRC	8.689	-	0.3624		
222-128918	V0383 Her	17 16 28.23	+20 58 44.0	RRC	RRAB	15.960	0.39722	0.56801		
223-112419	CM Leo	11 56 14.22	+21 15 30.2	RRAB	RRC	13.934	0.361732	-		
226-112429	BU Boo	14 01 42.58	+22 30 15.6	RRAB	RRC	14.853	0.445	0.4451		
227-103944	AH Leo	11 05 05.30	+23 21 09.0	RR	RRAB <sup>a</sup>	14.717	-	0.4663		
227-118042	V0682 Her	16 12 19.89	+23 19 34.7	RR	RRC	15.783	-	0.3102		
236-044458	IY Tau	05 42 23.13	+27 56 47.6	RRAB	RRC <sup>c</sup>	12.650	0.3764897	0.37651		
237-126582	V0864 Her	16 59 00.56	+28 04 54.7	RRC:	RRC	15.109	-	0.37537		
238-104806	NW UMa	11 16 55.26	+28 33 34.3	RRAB:	RRAB	15.650	0.5896	0.5895		
240-107056	VZ UMa	11 17 28.28	+29 40 30.1	RR	RRAB	14.452	-	0.5154		
248-106642	AT CVn	12 18 17.05	+33 39 56.0	RRAB:	RRC	15.060	-	0.3585		
276-118718	BN CVn	12 29 36.75	+47 49 17.3	RR:	RRAB	12.609	-	0.56365		
279-110274	DT UMa	08 53 44.85	+49 18 40.1	RR	RRC	15.787	-	0.32114		
282-141956	V1104 Cyg	19 18 00.49	+50 45 17.8	RR	RRAB	14.797	0.43626	0.43639		
283-142638	V1127 Cyg	19 32 05.81	+51 17 48.8	RR	RRAB	15.536	-	0.64727		
284-142523	V1116 Cyg	19 24 03.28	+51 39 52.6	RR	RRAB	15.493	-	0.53853		
285-135326	CD Dra	18 54 51.52	+52 28 45.1	RR	RRAB	16.147	-	0.5699		
286-140138	V1118 Cyg	19 24 42.97	+52 32 50.8	RR	RRAB	15.860	-	0.50654		
287-136993	V1106 Cyg	19 19 01.50	+53 25 15.8	RR	RRAB	15.160	2.04	0.40764		
294-139890	CI Dra	19 25 32.47	+56 43 32.4	RR	RRAB	16.243	-	0.47089		
300-132253	CY Dra	19 46 05.23	+59 34 26.3	RR:	RRAB	12.775	-	0.53494		

<sup>a</sup>Clearly exhibits the Blazhko effect in our data.

<sup>b</sup>Not listed in the set of known Galactic field Blazhko RR Lyrae stars from Skarka (2013).

<sup>c</sup>The light curve has a strange shape for an RR Lyrae star. However, the period and amplitude are consistent with an RRC classification.

and our period estimates (e.g. 3UC204-103494). Note that the GCVS period estimates are the best periods available for the other 416 RR Lyrae variables in our sample. We clearly detect the Blazhko effect in ten of the variables listed in Table 4 and this is the first detection of the effect in seven of them (see Skarka 2013). For 3UC188-089887, 3UC192-101314, 3UC209-135992 and 3UC234-000057, we measure Blazhko periods of  $69.7 \pm 0.5$ ,

$56.6 \pm 0.7$ ,  $38.8 \pm 0.2$  and  $80 \pm 4$  d, respectively, using the power spectrum analysis described in Section 4.5. For 3UC232-112040 and 3UC282-145093 we place lower limits of 100 and 80 d, respectively, on the Blazhko periods.

#### 4.5 New detections of the Blazhko effect in RR Lyrae stars

Finally, while inspecting the light curves of the remaining 499 RR Lyrae stars in our sample, we looked for clear indications of amplitude and phase modulations that characterise the Blazhko effect. We then checked our suspected Blazhko RR Lyrae stars against the catalogue of known Galactic field Blazhko stars in Skarka (2013). We found 27 RR Lyrae stars which clearly exhibit the Blazhko effect and which are not in the Skarka (2013) catalogue. This brings the total number of RR Lyrae stars where we have detected the Blazhko effect for the first time to 38 when taking into account the 4 and 7 such stars listed in Tables 2 and 4, respectively. We confirmed the presence of the Blazhko effect in 19 of these 27 variables by analysing the power spectra of the light curves using `period04`. We did this by prewhitening the power spectrum for the primary frequency  $f_0$  (and the harmonics where necessary) and considered the Blazhko effect to have been detected in the power spectrum if the next highest peak  $f_{\text{peak}}$  has a significant amplitude ( $>0.02$ - $0.05$  mag depending on light curve quality) and a ratio to the primary frequency in the range  $\sim 0.95$ - $1.05$  (Benkő, Szabó & Paparó 2011). The Blazhko period is then estimated via  $P_{\text{bl}} = 1/|f_{\text{peak}} - f_0|$ . We present the details of these Blazhko variables in Table 5 and we plot the phased light curves in Figure 8. In four cases where we could not estimate the Blazhko period from the power spectrum, we were still able to place lower limits on the Blazhko period by inspecting the unphased light curve.

#### 4.6 Electronic light curve data

We provide the 1783 light curves for the sample of 588 photometrically variable objects described in this paper in an electronic table. The 588 variables breakdown by type as follows: 482 RRAB, 78 RRC, 7 RR(B), 13 EW, 1 EA, 1 RS, 1 IA, 3 DCEP, 1 DCEPS and 1 CWB. An excerpt from the electronic table is presented in Table 6. The light curves will also be made available via CDS (Strasbourg) where we hope that the data will be of further use to the astronomical community.

ACKNOWLEDGMENTS: This research made use of the SIMBAD database, the VizieR catalogue access tool, and the cross-match service provided by CDS, Strasbourg, France. This publication was made possible by NPRP grant # X-019-1-006 from the Qatar National Research Fund (a member of Qatar Foundation). The statements made herein are solely the responsibility of the authors. AAF is grateful to DGAPA-UNAM for grant number IN104612. Thanks goes to Noe Kains at STScI in Baltimore for hosting the first author during part of this work and for the many useful discussions.

References:

- Alard C.; & Lupton R.H. 1998, *ApJ*, **503**, 325  
 Alsubai K.A.; Parley N.R.; Bramich D.M.; Horne K.; Collier Cameron A.; West R.G.; Sorensen P.M.; Pollacco D.; Smith J.C.; & Fors O. 2013, *Acta Astronomica*, **63**, 465  
 Alsubai K.A. et al. 2011, *MNRAS*, **417**, 709  
 Andrievsky S.M.; Kovtyukh V.V.; Wallerstein G.; Korotin S.A.; & Huang W., *PASP*, **122**, 877

- Belloni T.; Verbunt F.; & Mathieu R.D. 1998, *A&A*, **339**, 431  
 Benkó J.M.; Szabó R.; & Paparó M. 2011, *MNRAS*, **417**, 975  
 Bernhard K. 2010, *BAV Rundbrief 2/2010*, **59**, 78  
 Blazhko S. 1907, *Astronomische Nachrichten*, **175**, 325  
 Bramich D.M.; Horne K.; Albrow M.D.; Tsapras Y.; Snodgrass C.; Street R.A.; Hundermark M.; Kains N.; Arellano Ferro A.; Figuera Jaimes R.; & Giridhar S. 2013, *MNRAS*, **428**, 2275  
 Bramich D.M. 2008, *MNRAS*, **386**, 77  
 Bryan M.L. et al. 2012, *ApJ*, **750**, 84  
 Burke E.W.; Rolland W.W.; & Boy W.R. 1970, *Journal of the Royal Astronomical Society of Canada*, **64**, 353  
 Cox A.N.; Hodson S.W.; & Clancy S.P. 1983, *ApJ*, **266**, 94  
 Dworetzky M.M. 1983, *MNRAS*, **203**, 917  
 Gomez-Forrellad J.M.; & Garcia-Melendo E. 1995, *IBVS*, No. 4247  
 Lenz P.; & Breger M. 2005, *Communications in Asteroseismology*, **146**, 53  
 Mathieu R.D.; van den Berg M.; Torres G.; Latham D.; Verbunt F.; & Stassun K. 2003, *AJ*, **125**, 246  
 Moskalik P. 2014, *Proceedings of the International Astronomical Union*, **301**, 249  
 O’Connell D.J.K. 1951, *Riverview College Observatory Publications*, **2**, 85  
 Samus N.N. et al. 2009, *General Catalogue of Variables Stars (Vol. I-III, version 30/04/2013)*, **2009yCat....102025S**  
 Schmidt E.G. & Gross B.A. 1990, *PASP*, **102**, 978  
 Skarka M. 2013, *A&A*, **549**, 101  
 van den Berg M.; Stassun K.G.; Verbunt F.; & Mathieu R.D. 2002, *A&A*, **382**, 888  
 Vieira S.L.A. et al. 2003, *AJ*, **126**, 2971  
 Wallerstein G.; Kovtyukh V.V.; & Andrievsky S.M. 2009, *ApJ*, **692**, 127  
 Wils P.; Lloyd C.; & Bernhard K. 2006, *MNRAS*, **368**, 1757  
 Zacharias N. et al. 2010, *AJ*, **139**, 2184

**Table 3.** Double-mode RR Lyrae stars in our sample that are pulsating simultaneously in the fundamental and first overtone modes. In column 9, we list the fundamental and first overtone periods  $P_0$  and  $P_1$ , respectively, along with the period ratio  $P_1/P_0$  that we measure from our data. These periods are precise to the last decimal place quoted.

UCAC3 ID	GCVS ID	RA		Dec.		Variable Type		UCAC3 Ap. Mag	Period (d) GCVS	Period (d) This Work : $P_0, P_1, P_1/P_0$
		(J2000.0)	(J2000.0)	(J2000.0)	(J2000.0)	GCVS	This Work			
173-108416	V0500 Hya	08 47 46.93	-03 39 00.3	RR(B)	RR(B)	10.661	0.42079	0.5639, 0.4208, 0.7462		
183-255136	QW Aqr	21 07 26.08	+01 10 17.6	RR(B)	RR(B)	13.794	0.35498	0.4772, 0.3551, 0.7441		
201-119785	AQ Leo	11 23 55.28	+10 18 59.1	RR(B)	RR(B)	12.679	0.5497508	0.5498, 0.4102, 0.7461		
206-276118	CF Del	20 23 31.36	+12 59 30.5	RR	RR(B)	14.307	0.49923	0.47843, 0.35604, 0.74418		
218-133356	V0458 Her	17 08 30.92	+18 31 14.3	RRC	RR(B)	13.305	0.3599801	0.48352, 0.35998, 0.74450		
248-100379	WY LMi	09 30 23.25	+33 53 10.6	RRAB	RR(B)	15.391	0.420003	0.4923, 0.3662, 0.7439		
263-117859	BN UMa	11 16 22.91	+41 14 01.4	RRC	RR(B)	13.787	0.399901	0.53594, 0.39965, 0.74571		

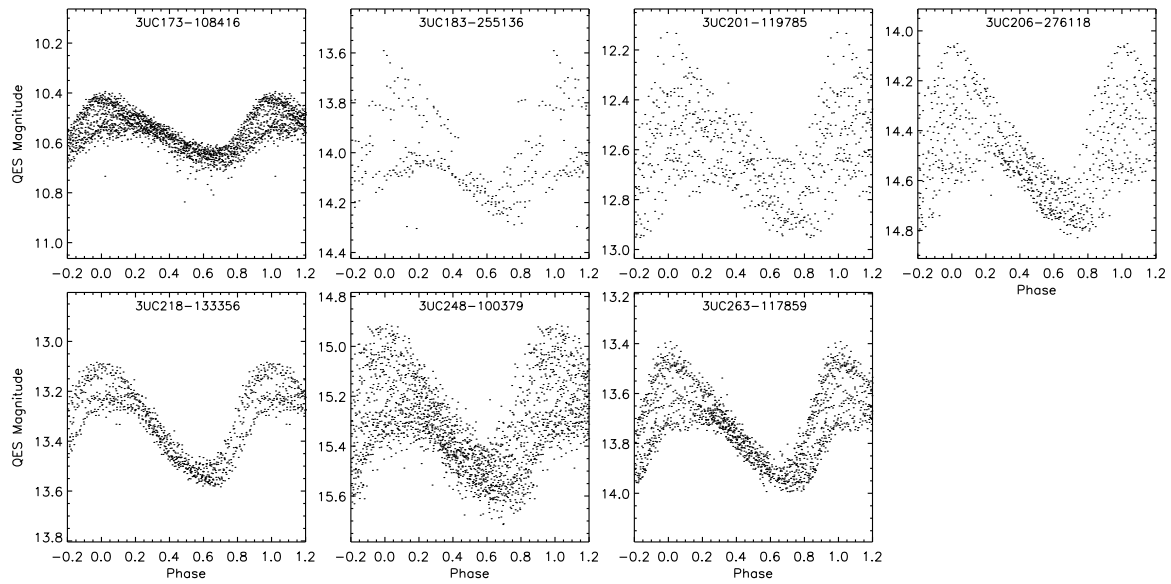


**Figure 7.** Phased light curves of the double-mode RR Lyrae stars. The light curves are phased with the first overtone period. The magnitude range in each plot is 1.0 mag.

**Table 4.** RR Lyrae stars with improved periods. Our periods are precise to the last decimal place quoted.

UCAC3 ID	GCVS ID	RA (J2000.0)	Dec. (J2000.0)	Variable Type	UCAC3		Period (d)	
					Aperture Mag	GCVS	This Work	
170-106909	DG Hya	08 58 06.36	-05 26 25.2	RRAB	12.569	0.429973	0.75425	
173-130413	HR Vir	13 42 28.63	-03 37 32.7	RRAB	14.414	-	0.7394	
176-019652	V0964 Ori	05 07 54.52	-02 08 48.7	RRAB	13.267	0.5046561	0.50464	
177-017006	V1830 Ori	04 49 34.97	-01 42 19.5	RRC	15.955	0.276438	0.2734	
177-261611	V0910 Aql	20 23 11.69	-01 33 57.5	RRAB	14.725	1.0	0.50019	
179-018625	V1844 Ori	05 03 36.84	-00 59 57.1	RRAB	15.057	0.778216	0.58908	
179-140408	V0694 Oph	16 22 47.53	-00 49 37.5	RRAB	14.845	0.62	0.6207	
179-141655	V0714 Oph	16 30 03.08	-00 59 56.5	RRAB	14.543	0.556	0.5557	
182-001386	BF Cet	00 27 03.97	+00 40 30.3	RRC	13.856	-	0.38034	
188-089887	CW Hya	08 55 07.81	+03 39 24.7	RRAB <sup>a,b</sup>	15.904	0.4820734	0.48050	
192-101314	V0430 Hya	09 04 48.58	+05 30 08.3	RRAB <sup>a,b</sup>	12.803	0.49691	0.496830	
193-135481	V2509 Oph	16 51 29.85	+06 22 26.2	RRAB	13.352	-	0.7786	
194-125256	GT Vir	14 56 48.38	+06 48 27.7	RRAB	15.089	0.4080564	0.68931	
195-285152	LX Del	20 52 18.98	+07 08 46.8	RRAB	13.876	-	0.5669	
197-007736	BP Cet	02 24 52.15	+08 24 05.0	RRAB	14.897	-	0.6924	
197-143679	V1013 Her	16 24 49.66	+08 04 14.1	RRAB	13.258	-	0.6448	
199-293401	LW Del	20 38 27.40	+09 12 05.4	RRAB	12.890	-	0.5811	
200-000971	FF Psc	00 17 48.58	+09 53 22.1	RRAB	12.441	0.70119	0.70110	
201-029115	V0944 Ori	05 36 11.40	+10 29 23.0	RRAB	15.456	-	0.5873	
201-114082	DL Leo	09 43 03.58	+10 19 01.3	RRAB	13.551	-	0.67378	
203-295430	DG Del	20 35 44.20	+11 28 09.0	RRAB	15.797	0.326961	0.4905	
203-295942	DI Del	20 36 49.52	+11 20 21.9	RRAB	15.487	0.367221	0.5803	
204-103494	AM Cnc	08 56 14.84	+11 37 20.6	RRAB	14.815	0.557615	0.55803	
204-113713	GP Leo	11 45 45.53	+11 52 08.5	RRAB	13.952	-	0.6793	
204-293402	HV Del	20 33 19.53	+11 32 01.7	RRAB	15.636	0.721265	0.5649	
207-115598	LL Leo	11 30 53.62	+13 19 28.4	RRAB	13.144	0.3324	0.33239	
209-135992	V1124 Her	17 04 32.86	+14 26 32.7	RRAB <sup>a</sup>	12.426	0.551	0.55103	
211-103053	KW Cnc	08 40 47.96	+15 24 52.4	RRAB	14.591	0.60102	0.60044	
211-128841	AW Ser	16 06 28.79	+15 22 05.8	RRAB	12.983	0.597097	0.597114	
211-291434	CS Del	20 28 54.87	+15 13 14.0	RRC	12.912	0.365737	0.37088	
212-310112	V0398 Peg	21 08 57.95	+15 56 55.3	RRAB	13.893	0.55259	0.55136	
213-110778	HY Com	12 18 16.02	+16 09 15.9	RRC	10.281	-	0.4488	
214-112667	BX Leo	11 38 02.06	+16 32 36.2	RRC	11.771	0.36286	0.36277	
215-288176	CH Del	20 23 18.39	+17 06 13.5	RRC	13.176	0.4596	0.31499	
216-128398	V0686 Her	16 14 23.25	+17 56 35.2	RRAB	14.800	0.510987	0.511004	
216-129723	V0695 Her	16 25 58.65	+17 42 52.0	RRAB <sup>a,b</sup>	14.574	0.678788	0.67884	
216-339177	V0611 Peg	23 46 41.17	+17 38 02.6	RRAB	13.794	0.58868	0.588665	
216-339421	V0419 Peg	23 50 05.03	+17 53 44.0	RRAB	14.674	0.60373	0.60370	
218-287254	EO Del	20 37 47.72	+18 55 30.6	RRAB	14.378	0.580861	0.57990	
219-270870	II Del	20 50 01.18	+19 11 43.5	RRC	14.558	0.408021	0.4078	
224-130750	SW Her	16 58 27.56	+21 32 51.5	RRAB	14.956	0.49287277	0.492861	
225-123239	V0504 Ser	16 01 52.29	+22 22 47.9	RRAB	14.169	0.56396	0.563833	
225-131962	V0382 Her	17 16 17.21	+22 01 04.5	RRAB	15.934	0.4556118	0.45554	
225-265413	FH Vul	20 40 19.89	+22 13 24.3	RRAB	13.267	0.4054185	0.405412	
227-031814	HX Tau	05 10 48.79	+23 12 22.7	RRAB	15.298	0.53875	0.53826	
227-119598	V0362 Her	16 30 39.55	+23 26 41.7	RRAB	14.791	0.718297	0.7185	
228-098638	EZ Cnc	08 52 57.67	+23 47 54.2	RRAB	12.404	-	0.54578	
228-261882	BL Peg	21 22 59.51	+23 53 32.1	RRAB <sup>a,b</sup>	14.433	0.55543	0.55555	
229-254073	V0507 Vul	20 49 45.85	+24 12 44.9	RRC	11.848	0.336126	0.33607	
230-118556	V0677 Her	16 08 04.15	+24 59 20.2	RRAB	14.387	0.475716	0.475728	
230-120541	V1186 Her	16 29 14.78	+24 59 38.7	RRAB	13.894	0.44032	0.44025	
231-126743	V0467 Her	17 12 50.79	+25 01 48.6	RRAB	14.850	0.6835066	0.65352	
232-094191	AS Cnc	08 25 42.16	+25 43 08.5	RRAB	12.998	0.61752	0.61754	
232-096427	SX Cnc	08 51 19.58	+25 33 24.3	RRAB	14.026	0.5101754	0.51016	
232-111124	IY Boo	14 19 39.22	+25 47 24.1	RRAB	14.462	0.59165	0.59171	
232-112040	LN Boo	14 37 09.05	+25 44 46.6	RRAB <sup>a,b</sup>	13.997	0.46675	0.46667	
234-000057	GV Peg	00 00 35.59	+26 39 49.5	RRAB <sup>a,b</sup>	13.600	0.5669237	0.56607	
235-118691	CT CrB	16 18 34.34	+27 28 13.2	RRAB <sup>a</sup>	14.271	0.508646	0.50858	
236-097672	KV Cnc	08 40 02.43	+27 43 31.5	RRAB <sup>a</sup>	12.916	0.502	0.5020	
236-123949	V0860 Her	16 50 38.71	+27 58 40.3	RRAB	16.051	-	0.57083	
237-108110	EF Leo	11 49 10.95	+28 00 25.6	RRAB	15.891	-	0.5979	
237-274829	V0466 Vul	21 05 22.87	+28 17 49.4	RRAB	14.752	0.4759	0.47592	
239-000617	IQ Peg	00 06 05.70	+29 19 12.6	RRAB	16.319	-	0.47993	
240-120704	RV CrB	16 19 25.85	+29 42 47.6	RRC	11.387	0.331565	0.33172	
245-013999	VX Tri	02 10 00.87	+32 24 08.9	RRAB	14.576	-	0.6331	
247-105751	CK Com	12 14 50.60	+33 06 05.9	RRAB	14.727	0.6939962	0.6938	
248-104694	V0345 UMa	11 17 49.43	+33 40 14.8	RRAB	14.434	0.57667	0.57662	
248-106344	DN CVn	12 09 17.00	+33 39 35.5	RRC	15.083	0.3266873	0.32625	
251-289738	DM And	23 32 00.72	+35 11 48.9	RRAB	11.978	0.630387	0.6305	
254-099280	VY LMi	09 27 41.32	+36 58 22.4	RRAB	13.838	-	0.52614	
255-095249	DQ Lyn	08 23 40.99	+37 28 10.8	RRC	11.670	-	0.4949	
257-098638	EN Lyn	08 46 07.04	+38 02 52.7	RRAB	13.554	0.6249	0.6251	
262-118704	AO UMa	11 07 39.83	+40 33 57.2	RRAB	15.749	0.561614	0.56265	
263-257028	DY And	23 58 42.21	+41 29 19.4	RRAB	13.674	0.603087	0.60323	
266-126680	AQ UMa	11 12 59.53	+42 48 41.7	RRAB	16.369	0.644029	0.6433	
266-127186	AV UMa	11 29 40.53	+42 44 24.7	RRAB	15.935	0.479483	0.47911	
272-115635	AX UMa	11 38 26.84	+45 56 05.9	RRAB	13.591	0.53491	0.53468	
278-047793	AN Per	03 08 31.34	+48 32 40.4	RRAB	14.367	0.602818	0.6021	
282-136249	DT Dra	18 49 57.25	+50 35 12.8	RRAB	13.625	-	0.52664	
282-145093	V1949 Cyg	19 30 12.47	+50 48 21.2	RRAB <sup>a,b</sup>	13.714	-	0.4994	
293-139097	XZ Cyg	19 32 29.31	+56 23 17.5	RRAB	9.500	0.4667	0.4666	
297-143410	V1035 Cyg	20 05 41.44	+58 02 48.9	RRAB	15.798	0.5321	0.5318	

**Table 5.** New detections of the Blazhko effect in Galactic RR Lyrae stars. These stars are not listed in the catalogue of Skarka (2013).

UCAC3 ID	GCVS ID	RA	Dec.	Variable Type	UCAC3	Period (d)	Blazhko Period (d)
		(J2000.0)	(J2000.0)		Aperture Mag	GCVS	
162-283238	PQ Aqr	20 43 15.75	-09 09 28.7	RRAB	13.713	0.512286	-
164-130527	V0574 Vir	14 34 30.48	-08 18 32.7	RRAB	14.529	0.47439	26.3±0.3
172-132806	V0586 Vir	14 39 47.52	-04 08 05.3	RRAB	13.376	0.682772	132±3
174-136150	V0585 Vir	14 39 27.36	-03 27 36.6	RRAB	12.872	0.601615	93.8±0.4
174-247961	PS Aqr	20 44 03.69	-03 23 12.3	RRAB	14.411	0.59102	-
175-104590	V0486 Hya	08 30 29.83	-02 42 36.8	RRAB	13.107	0.508655	18.5±1.0
176-131910	MS Lib	14 53 32.99	-02 06 51.5	RRAB	14.445	0.441448	105±10
178-129959	V0561 Vir	14 28 40.65	-01 27 59.4	RRAB	15.893	0.550276	42.0±0.6
186-091699	V0487 Hya	08 32 57.03	+02 59 02.9	RRAB	13.447	0.561485	64.4±0.3
186-092895	GL Hya	08 40 59.22	+02 37 22.2	RRAB	13.409	0.50593	157±10
193-094864	V0425 Hya	08 20 51.78	+06 28 24.2	RRAB	14.829	0.5508	61.1±0.2
194-123163	AF Vir	14 28 09.82	+06 32 43.9	RRAB	11.507	0.48376	35±5
201-137842	V1162 Her	16 17 00.49	+10 17 27.9	RRAB	13.429	0.547925	-
204-017429	V1327 Tau	04 40 09.89	+11 43 17.0	RRC	13.169	0.3312	23.7±0.3
206-121944	UY Boo	13 58 46.34	+12 57 06.5	RRAB	11.001	0.6508964	-
208-001501	FI Psc	00 23 22.80	+13 45 40.8	RRAB	13.590	0.53129	>120
209-121247	LS Boo	14 38 21.77	+14 24 55.1	RRAB	13.624	0.5527108	42.9±1.9
216-112989	AE Leo	11 26 12.19	+17 39 39.7	RRAB	12.508	0.626723	62±4
216-121383	LW Boo	14 40 32.61	+17 35 57.3	RRAB	13.434	0.56342	63.9±0.6
217-331820	V0606 Peg	23 41 58.75	+18 13 01.4	RRAB	12.564	0.52966	26.7±0.3
228-114655	DD Boo	14 51 20.08	+23 32 30.0	RRC <sup>a</sup>	12.889	0.3393397	9.64±0.02
237-128729	V0385 Her	17 16 26.66	+28 05 56.4	RRAB	15.499	0.5281428	>100
238-035854	NU Aur	05 09 02.37	+28 40 52.7	RRAB	13.436	0.53941672	>60
239-115076	XX Boo	14 51 37.56	+29 21 26.7	RRAB	12.061	0.581402	148±7
248-099777	FW Lyn	09 19 51.49	+33 52 23.9	RRAB	13.650	0.52174	>110
296-130079	NQ Dra	18 44 13.17	+57 40 59.4	RRAB	13.752	0.52919	34.5±0.4
304-116701	V0429 Dra	19 59 32.15	+61 31 21.0	RRAB	14.994	0.5862	87.0±2.2

<sup>a</sup>Although the amplitude modulations are small, they are clear to the eye in the unphased light curve and they are strongly detected in the power spectrum. To help confirm our conclusions for this star, we checked the literature and found that Gomez-Forrellad & Garcia-Melendo (1995) also suspected this star of exhibiting the Blazhko effect.

**Table 6.** Time-series photometry for the 588 variable stars described in this paper.

The epoch of mid-exposure (heliocentric Julian date) is listed in column 4. The magnitudes in column 5 are calibrated QES magnitudes. Column 6 contains the uncertainties on the magnitudes. The light curve identifier string is listed in column 7 and consists of a concatenation of the target field name, a camera identifier and an observing campaign identifier.

UCAC3 ID	GCVS ID	Variable Type	HJD (d)	$m$ (mag)	$\sigma_m$ (mag)	Light Curve Identifier
3UC161-102683	DH Hya	RRAB	2455639.60565	12.265	0.256	084014-044854_416_C5
3UC161-102683	DH Hya	RRAB	2455639.61285	12.347	0.262	084014-044854_416_C5
⋮	⋮	⋮	⋮	⋮	⋮	⋮
3UC161-102683	DH Hya	RRAB	2455639.61110	12.268	0.377	092014-044854_416_C5
3UC161-102683	DH Hya	RRAB	2455639.61810	12.296	0.380	092014-044854_416_C5
⋮	⋮	⋮	⋮	⋮	⋮	⋮
3UC162-107613	SZ Hya	RRAB	2455229.77350	11.529	0.076	091000-071400_403_C2
3UC162-107613	SZ Hya	RRAB	2455229.78082	11.427	0.045	091000-071400_403_C2
⋮	⋮	⋮	⋮	⋮	⋮	⋮

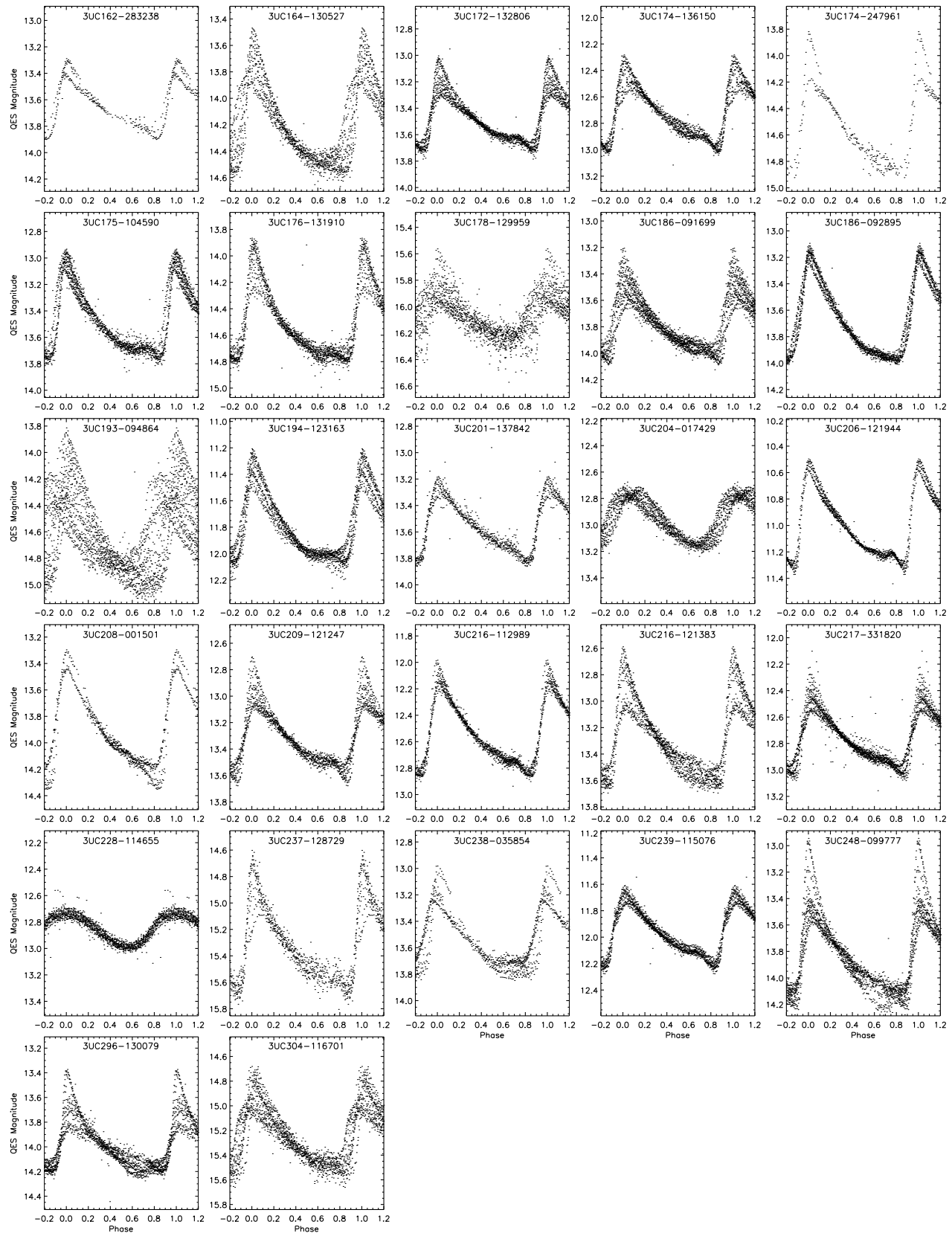


**Figure 8.** Phased light curves of the RR Lyrae stars exhibiting the Blazhko effect and that are not in the catalogue of Skarka (2013). The magnitude range in each plot is 1.4 mag.